

## Associated charm production and correlations between multileptons in (anti)neutrino interactions

J. Smith and G. Valenzuela

*Institute for Theoretical Physics, State University of New York at Stony Brook, Stony Brook, New York 11794*

(Received 24 March 1983)

Associated charm production and decay in (anti)neutrino interactions has often been proposed to explain the (anti)neutrino like-sign dimuon events. We show that a particular phenomenological model of  $c\bar{c}$  production and decay is also capable of explaining both the  $\mu^-e^-$  events seen recently in bubble-chamber experiments and a specific fraction of the neutrino-induced trimuon events. The correlations between these different reaction channels strengthen the conclusion that  $c\bar{c}$  pairs are formed in approximately 1% of all deep-inelastic (anti)neutrino interactions.

### I. INTRODUCTION

The study of multilepton events in (anti)neutrino interactions has led to a detailed understanding of heavy-quark production and decay mechanisms. For instance, the neutrino-induced opposite-sign  $\mu^-\mu^+$  and  $\mu^-e^+$  events are well explained by the production and decay of particles carrying the charm quantum number. The same model explains the  $\mu^+\mu^-$  and  $\mu^+e^-$  events seen in the antineutrino interactions. In contrast, however, there has been a steady accumulation over the past few years of neutrino-induced like-sign  $\mu^-\mu^-$  and  $\mu^-e^-$  events, which, together with  $\mu^+\mu^+$  and  $\mu^+e^+$  events in antineutrino interactions, are not so well understood as the opposite-sign events.<sup>1-3</sup>

The production rates for the like-sign dimuon events are small, making it difficult to extract a signal from the background. The fact that the experiments had different spectra, targets, and cuts makes it very tricky to directly compare the rates. The situation has been improved, however, by the publication of high-statistics data from the Amsterdam-CERN-Hamburg-Moscow-Rome (CHARM) experiment in the paper of Jonker *et al.*<sup>1</sup> On the basis of  $74 \pm 17 \mu^-\mu^-$  and  $295 \pm 32 \mu^-\mu^+$  events induced in a  $\nu_\mu$  beam, they reported  $\sigma(\mu^-\mu^-)/\sigma(\mu^-\mu^+) = 0.14 \pm 0.07$ . Also from  $52 \pm 13 \mu^+\mu^+$  and  $285 \pm 29 \mu^+\mu^-$  events induced in a  $\bar{\nu}_\mu$  beam, they reported that  $\sigma(\mu^+\mu^+)/\sigma(\mu^+\mu^-) = 0.18 \pm 0.09$ . Although the errors are still large, there can no longer be any doubt that like-sign muons are produced in (anti)neutrino interactions, and a theoretical understanding of their origin is necessary.

Bubble-chamber experiments have also identified  $\mu^-e^-$  events in neutrino interactions and  $\mu^+e^+$  events in antineutrino interactions. The recent analysis by Haatuft *et al.*<sup>2</sup> of Gargamelle data yielded ten  $\mu^-e^-$  events where the momentum of the muon was greater than 4.5 GeV/c and the momentum of the electron was greater than 0.5 GeV/c. They reported a rate relative to charged-current events of  $(6.7 \pm 3.9) \times 10^{-4}$ . Four antineutrino-induced  $\mu^+e^+$  events were reported in the paper of Ammosov *et al.*,<sup>3</sup> giving a rate of  $(4.8^{+5.3}_{-3.2}) \times 10^{-4}$  relative to

charged-current events.

Various explanations of the like-sign dilepton events have been discussed in the literature. The interested reader should consult the theoretical papers on the subject listed in Refs. 4 and 5. For completeness, we have also given a compilation of review talks in Ref. 6. The most promising explanation of these events is that they signal the production of  $c\bar{c}$  pairs in charged-current (anti)neutrino events. Hence, there is one "leading" lepton from the primary interaction and a second lepton produced in the semileptonic decay of one of the charmed particles. However, no one has managed to calculate the  $c\bar{c}$  production rate from first principles. This means that the comparison between theory and experiment is limited to the distributions for the leptons with the normalization given by the experimental rate. Recently, Godbole and Roy<sup>5</sup> made a comparison between the experimental data of the CHARM collaboration and the results of a phenomenological  $c\bar{c}$  production model and obtained satisfactory agreement. We outline their model in Sec. II, since we wish to use it in the later parts of this paper, where we investigate its implications for the  $\mu^-e^-$  and trimuon events.

If  $c\bar{c}$  production and decay is the correct explanation of the like-sign events, then there is a well-defined rate for the charmed particles containing the  $c$  and  $\bar{c}$  quarks to decay into muons leading to trimuon events. A high rate for  $\sigma(\mu^-\mu^-)/\sigma(\mu^-)$  leads inevitably to a high rate for  $\sigma(\mu^-\mu^-\mu^+)/\sigma(\mu^-)$  and a potential conflict with well-established trimuon rates.<sup>7,8</sup> Since the majority of the trimuon events identified in the high-statistics experiment of the CERN-Dortmund-Heidelberg-Saclay (CDHS) collaboration<sup>8</sup> are explainable by other models, there has never been any convincing evidence for a  $c\bar{c}$  component in the trimuon signal. Therefore, we have always been somewhat sceptical of the large rates reported by some groups for  $\sigma(\mu^-\mu^-)/\sigma(\mu^-)$ . Recently, however, the CDHS collaboration<sup>9</sup> has reported the final results of a data analysis of 165  $\mu^-\mu^-\mu^+$  events produced in  $\nu_\mu$  beams and 33  $\mu^+\mu^-\mu^+$  events produced in  $\bar{\nu}_\mu$  beams. The distributions in the invariant masses of the secondary  $\mu^-\mu^+$  pairs are too broad to be explained by the standard trimuon-

production models alone. As we will show in Sec. III, it is possible to correlate this observation with the presence of an additional component from  $c\bar{c}$  production and decay. Hence, this measurement is consistent with the  $c\bar{c}$  explanation of the  $\mu^-\mu^-$  and  $\mu^+\mu^+$  events. This type of correlation was proposed earlier by Kane, Smith, and Vermaseren<sup>4</sup> but, at that time, there were not enough trimuon events to see such an effect.

An additional confirmation of the  $c\bar{c}$  production and decay model is the satisfactory explanation of the rates and distributions for the  $\mu^-e^-$  events reported recently by Haatuft *et al.*<sup>2</sup> Since the cuts on the electron energy are much lower than the typical cuts on the muon energy (0.3–0.8 GeV versus 4–9 GeV), the  $\mu^-e^-$  rates are sensitive to a wider range of kinematic variables. As we will show in Sec. IV, there is good agreement between theory and experiment for the  $\mu^-e^-$  rates and distributions even though the event sample is small. The one negative comment one could make against a  $c\bar{c}$  explanation is that none of the events are accompanied by  $V^0$  decays. We will have to wait until the Columbia-BNL collaboration has finished the data analysis of new film from Fermilab to see whether this is just a statistical accident. We also note that the  $\mu^+e^+$  event rate reported by Ammosov *et al.*<sup>3</sup> fits the theoretical result from the  $c\bar{c}$  model.

## II. MODEL FOR LIKE-SIGN DIMUONS

The  $c\bar{c}$  model invoked to explain like-sign dimuon events has been used in two different ways. First, there have been attempts at rigorous calculations based on the use of first-order perturbation theory, where a  $c\bar{c}$  pair is produced via gluon radiation. This model fails to account for the large rate needed to fit the experimental data so it must be discarded. The second use of the  $c\bar{c}$  model is purely phenomenological. By this we mean that some ansatz is chosen for the  $c\bar{c}$  pair production cross section with parameters taken from other data. In such a model, the cross section is not normalized so it is adjusted to fit the experimental rate. We will follow this approach here and use a recent model of Godbole and Roy<sup>3</sup> since they have already demonstrated that it gives a reasonable fit to the like-sign dimuon rates and distributions. Our objective is to check that the model also fits the  $\mu^-e^-$  and  $\mu^+e^+$  rates without predicting too many  $\mu^-\mu^+\mu^-$  or  $\mu^-e^+e^-$  events.

The details of the Godbole-Roy model are given here for completeness. One assumes that the inclusive (anti)neutrino cross section is expressed in terms of quark distribution functions, so that

$$\frac{d^2\sigma^{(\nu,\bar{\nu})}}{dx dy} = \frac{G^2ME}{\pi} \left\{ \frac{1}{2} [2xF_1^{(\nu,\bar{\nu})}(x, Q^2) \pm xF_3^{(\nu,\bar{\nu})}(x, Q^2)] + \frac{1}{2}(1-y)^2 [2xF_1^{(\nu,\bar{\nu})}(x, Q^2) \mp xF_3^{(\nu,\bar{\nu})}(x, Q^2)] \right. \\ \left. + (1-y)[F_2^{(\nu,\bar{\nu})}(x, Q^2) - 2xF_1^{(\nu,\bar{\nu})}(x, Q^2)] \right\}. \quad (1)$$

The variables  $x$  and  $y$  are related to the invariant mass and momentum transfer by the standard formulas

$$\begin{aligned} v &= (W^2 - M_N^2 + Q^2)/2M_N, \\ x &= Q^2/2M_N v, \\ y &= v/E_\nu. \end{aligned} \quad (2)$$

The structure functions are defined via

$$\begin{aligned} F_2^{\nu}(x, Q^2) &= xF_3(x, Q^2) + A(\bar{s})(1-x)^{B(\bar{s})}, \\ F_1^{\nu}(x, Q^2) &= F_2(x, Q^2)/2x, \end{aligned} \quad (3)$$

and

$$F_3^{\nu}(x, Q^2) = 3x^{\eta_1(\bar{s})-1}(1-x)^{\eta_2(\bar{s})}/D(\bar{s}).$$

We only include the scaling deviations above  $Q^2=5$  (GeV/c)<sup>2</sup> so that, defining

$$\bar{s} = \begin{cases} 0, & Q^2 < 5 \text{ (GeV/c)}^2 \\ \ln \left[ \frac{\ln(Q^2/0.47)}{\ln(10.64)} \right], & Q^2 \geq 5 \text{ (GeV/c)}^2, \end{cases} \quad (4)$$

the parameters in (3) are given by

$$\begin{aligned} \eta_1 &= 0.56 - 0.147 \bar{s}, \\ \eta_2 &= 2.71 + 0.813 \bar{s}, \\ D(\bar{s}) &= 0.77 + 0.29 \bar{s}, \\ A(\bar{s}) &= 0.99 + 1.71 \bar{s}, \\ B(\bar{s}) &= 8.1 + 4.76 \bar{s}. \end{aligned} \quad (5)$$

Equations (1)–(5) specify completely the production of quarks (hadrons) in the (anti)neutrino final state. However, these are primarily  $u$ ,  $d$ ,  $\bar{u}$ , or  $\bar{d}$  quarks so we still need to add the probability that a  $c\bar{c}$  pair is formed.

In terms of the quark-parton model, we assume that the final quark in the (anti)neutrino interaction has a finite probability of producing a cluster of hadrons containing a  $c\bar{c}$  pair. The laboratory distribution of the actual charmed particles, which we assume to be  $D\bar{D}$  mesons, is given in terms of two variables,  $z$  and  $p_T$ . The former is the fractional energy of the cluster taken by the  $D$  meson and the latter is its transverse momentum with respect to the cluster direction. We assume that

$$\frac{d^2\sigma}{dz dp_T^2} = \frac{C}{z} \exp \left[ -\frac{1}{2} kM \left[ z + \frac{m_D^2 + p_T^2}{zM^2} \right] \right], \quad (6)$$

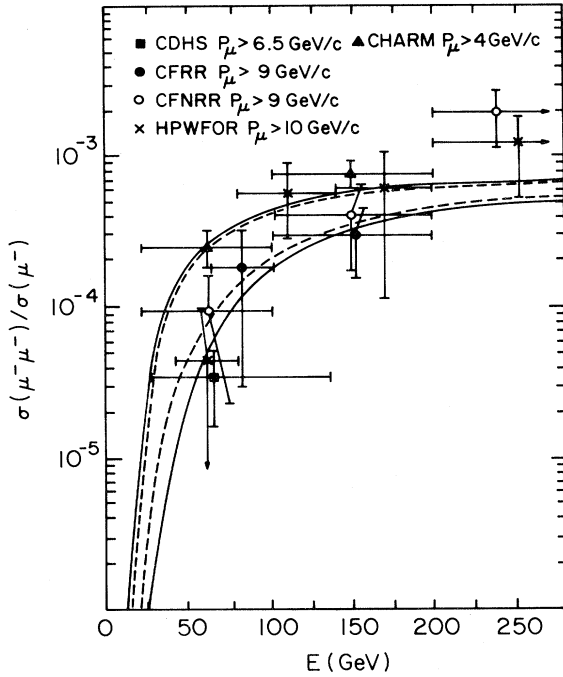


FIG. 1. The ratio  $\sigma(\mu^+\mu^-)/\sigma(\mu^-)$  as a function of the neutrino energy. The upper solid curve is the Godbole-Roy result and the upper dashed curve is our result for  $E_{\mu^-} > 4$  GeV. The lower solid curve is the Godbole-Roy result for  $E_{\mu^-} > 9$  GeV and agrees with the result of our computation. The lower dashed curve shows the effect of a threshold form factor on the  $E_{\mu^-} > 4$ -GeV results.

where  $M=5$  GeV and  $k=5$  GeV $^{-1}$ . This formula leads to a  $z$  distribution which is peaked near  $z=\frac{1}{2}$  and a sharply falling  $p_T$  spectrum.

The  $D$ -meson distribution is normalized by requiring that the integral over the region  $z_{\min} \leq z \leq z_{\max}$ ,  $0 \leq p_T^2 \leq 4$  GeV $^2$  be unity. With  $m_D=1.87$  GeV, the limits on  $z$  are 0.168 and 0.832, and the normalization constant  $C$  is  $1.87 \times 10^4$ . An upper limit on  $p_T^2$  of 4 GeV $^2$  is sufficient in view of the exponential fall-off in this variable. For example, if we extend the upper limit to 16 GeV $^2$ , then the normalization only changes by 1%.

Folding together Eqs. (1) and (6) requires a specification of the direction of the outgoing light-mass quark and the energy of the physical  $D$  meson,  $E_D$ . It is assumed that  $E_D = \nu z$  and the  $p_T$  in (6) is defined with respect to the charged-current ( $W$ -boson) direction. A normalization factor is then added to the product of (1) and (6) so that  $D\bar{D}$  pairs are produced in (anti)neutrino collisions at high energies with a 1/2% probability.

Finally, to complete the chain, we add on the decay of the  $D$  meson within the framework of a regular charged-current interaction  $\bar{c} \rightarrow \bar{s} + \mu^- + \nu_\mu$ .

We have normalized the decay rate to the standard  $\beta$ -decay rate

$$\Gamma = \frac{M_c^5}{192\pi^3} \gamma, \quad (7)$$

where

$$\gamma = (1 - \rho^2)[1 + \rho(\rho - 8)] - 12\rho^2 \ln \rho, \quad \rho = M_s^2/M_c^2, \quad (8)$$

is a correction factor to account for the large mass of the  $s$  quark. Then we have multiplied by the branching ratio for  $D$  leptonic decay which we took to be 20%.

With the parameters chosen above, we first independently rederived the results for the rates and distributions for  $\mu^-\mu^-$  events reported by Godbole and Roy and obtained excellent agreement. The prediction for the rate is reproduced in Fig. 1. Then we varied some of the parameters, such as the masses of the  $c$  and  $s$  quarks. In all cases, the results of the model were very insensitive to reasonable changes in the input parameters. Since the model successfully reproduces the features of the like-sign dimuon events, we now turn to the trimuon reaction to check that there is no inconsistency with rates and distributions for these events. In this part of the analysis, we concentrate on the neutrino data since there are many more  $\mu^-\mu^+\mu^-$  events than  $\mu^+\mu^+\mu^-$ .

### III. MODEL FOR TRIMUONS

The model we use for trimuon production in (anti)neutrino collisions is a straightforward iteration of the previous model. We randomly allow either a  $D$  or a  $\bar{D}$  meson to be produced at a specific  $z$  and  $p_T$ . Then we recompute the available energy left in the cluster. The other meson is then generated with another fraction of this energy and another  $p_T$  accommodate to the probability in (6). Hence, aside from the kinematical restrictions the  $D$  and  $\bar{D}$  mesons decay independently. This gives a model where there is usually one fast leading muon followed by a slower dimuon pair. Since the charge of the decay meson is chosen randomly, the latter muons have equal energies on the average.

The model discussed above cannot account for all the trimuon signal for the simple reason that its predictions do not accommodate the experimental data. Previous work on trimuon rates and distributions $^{7-9}$  indicate that at least a two-component model is needed to fit the experimental results. This conclusion was based primarily on the experimental rates and two important distributions. First, the azimuthal angle on the plane perpendicular to the neutrino beam between the  $p_T$  vector of the leading muon and the  $p_T$  vector for the sum of the other muon momenta, which we call  $\phi_{1(2+3)}$ . The experimental distribution in  $\phi_{1(2+3)}$  for 72 events published by the CDHS group $^8$  is shown in Fig. 2. The large peak near  $180^\circ$  is explained by a model where light-mass dimuons are produced in hadronic collisions, $^{8,10}$  while the small peak near  $0^\circ$  is explained by electromagnetic radiation of dimuon pairs. $^{11}$  Since both mechanisms involve the emission of pairs of muons of light mass, the distribution in the invariant mass of the secondary pair  $M_{23}$  shows a large enhancement at small masses. For interest, we reproduce the distribution for the CDHS events in Fig. 3. All the other distributions in the energies and angles of the muons were explainable on the basis of this two-component

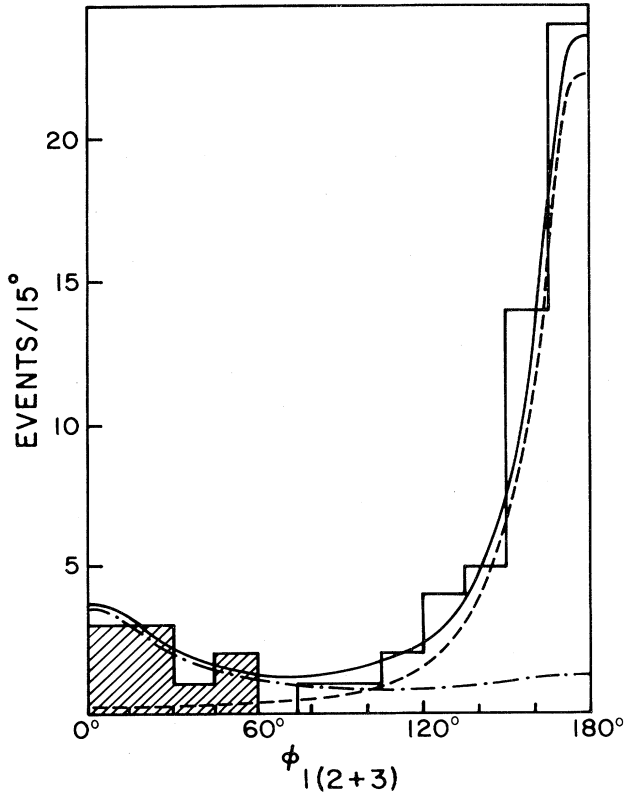


FIG. 2. The distribution in  $\phi_{1(2+3)}$  for the CDHS events reported in Ref. 8. The dot-dashed curve shows the electromagnetic contribution, the dashed curve the hadronic contribution, and the solid curve the sum of the two. The actual electromagnetic rate is normalized to the shaded events at small  $\phi_{1(2+3)}$ .

model. However we should remind the reader that the normalization of the hadronic component from the data on the reaction  $\pi N \rightarrow \mu^+ \mu^- X$  yielded too small a result.<sup>8-10</sup> Therefore the calculated rate for the hadronic component in the reaction  $\nu N \rightarrow \mu^- \mu^+ \mu^- X$  has been multiplied by a factor of 2.5.

What we would now like to exploit is a new feature becoming apparent in the final sample of 165  $\mu^- \mu^- \mu^+$  events accumulated in the CDHS experimental runs. The muon momenta are given in the thesis of Peyaud<sup>9</sup> and we reproduce the  $\phi_{1(2+3)}$  and  $M_{23}$  histograms in Figs. 4 and 5. The results of his calculations for the electromagnetic, hadronic, and total contributions are shown as dot-dashed, dashed, and solid curves, respectively. If one examines the figures carefully one notes that the peak in the hadronic distribution in Fig. 5 is at a higher value of  $M_{23}$  than the corresponding peak of Fig. 3. The reason for this is not clear but we speculate that it has to do with experimental smearing because three different beams were used to provide the experimental data in the figure. Although qualitatively Figs. 3 and 5 look the same, it is apparent that the dimuon mass distribution is too broad to be satisfactorily explained by the two-component picture, mentioned above. Another component is necessary to explain the events at large  $M_{23}$ . The  $c\bar{c}$  model can be invoked for this purpose

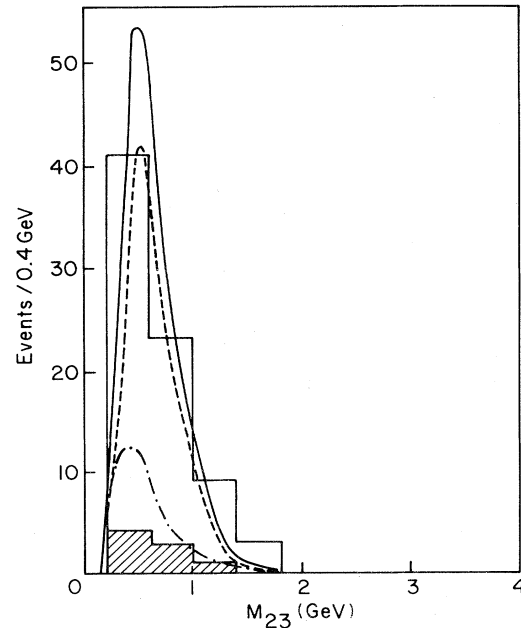


FIG. 3. The distribution in  $M_{23}$  for the CDHS events reported in Ref. 8. The notation is the same as in Fig. 2. The shaded events in Fig. 2 are reproduced as the shaded events shown here.

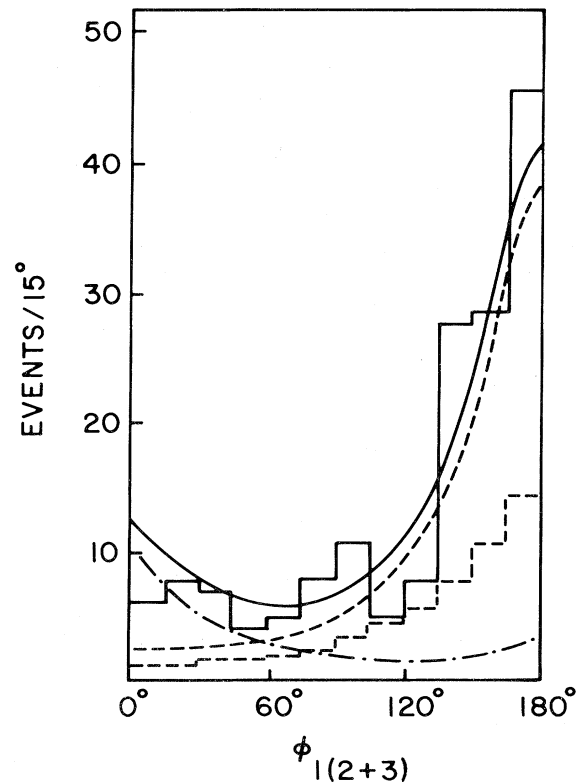


FIG. 4. The distribution in  $\phi_{1(2+3)}$  for all the available CDHS events reported in Ref. 9. The notation is the same as in Fig. 2. The dashed histogram shows the prediction of the  $c\bar{c}$  model which can account for  $\frac{1}{3}$  of the total rate.

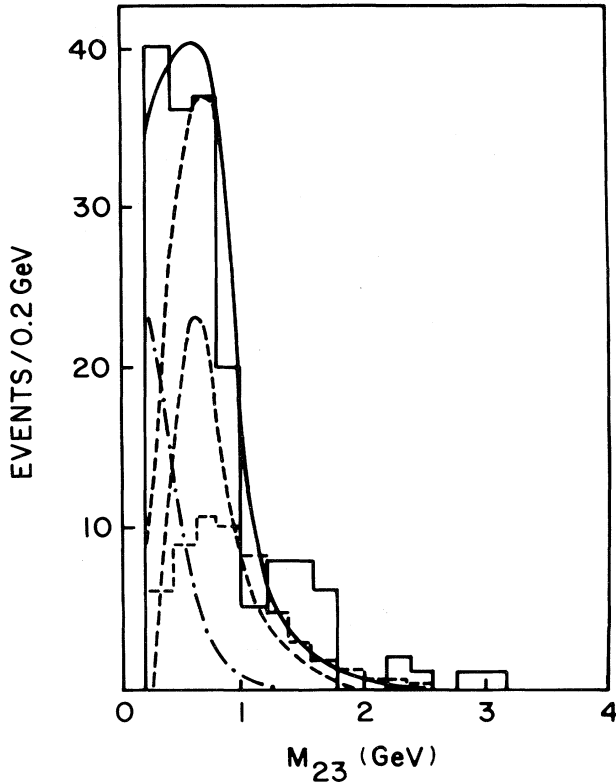


FIG. 5. The distribution in  $M_{23}$  for all the available CDHS events reported in Ref. 9. The notation is the same as Fig. 2. The dashed histogram shows the prediction of the  $c\bar{c}$  model which can account for  $\frac{1}{3}$  of the total rate.

since it gives a peak in the  $M_{23}$  distribution near  $M_{23}=0.8$  GeV. In fact, if we use the branching ratio of 20% and the  $c\bar{c}$  model in Sec. II we actually predict the dashed histogram in Fig. 5 for the 350-GeV beam at CERN. The corresponding trimuon rate is

$$\sigma(\mu^-\mu^+\mu^-, E_\mu > 4.5 \text{ GeV})/\sigma(\mu^-) = 1.0 \times 10^{-5}$$

which should be added to the rates predicted by the hadronic and electromagnetic components. The final rate is small but that is a reflection of the cuts in the muon energies. What we would like to propose, therefore, is that the hadronic component in the trimuon production cross section be reduced to its actual calculated rate by removing the enhancement factor of 2.5. Then the  $c\bar{c}$  component should be added to the other two components. This clearly allows a better fit to the  $M_{23}$  mass distribution. A readjustment of the magnitude of the hadronic component could run into conflict with the other trimuon distributions, but we have checked that there is no problem. In particular, as one can see from Fig. 4, the prediction of the  $\phi_{1(2+3)}$  distribution from the  $c\bar{c}$  model can clearly be added to the other curves once the scale factor in the hadronic component is removed.

The conclusion we reach is, therefore, that the trimuon

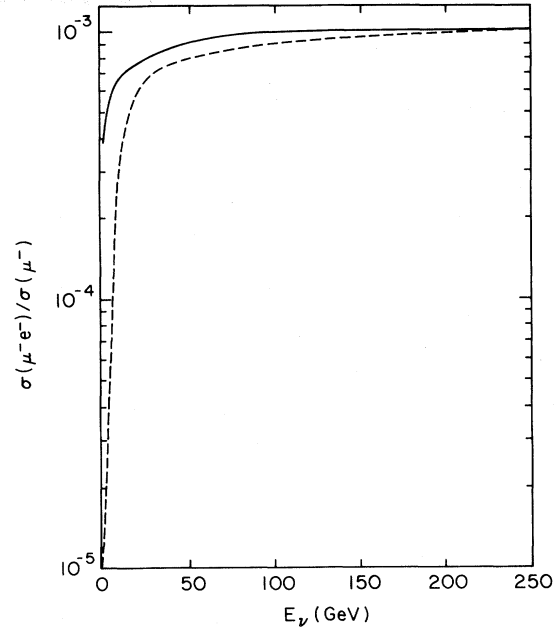


FIG. 6. The ratio  $\sigma(\mu^-e^-)/\sigma(\mu^-)$  as a function of the neutrino energy for, solid curve, a cut on the muon energy at 4 GeV and, dashed curve, a cut on the muon energy at 4 GeV and on the electron energy at 300 MeV.

events shown in Figs. 4 and 5 require a  $c\bar{c}$  component to obtain good agreement between theory and experiment. If we normalize the  $c\bar{c}$  rate to  $\frac{1}{2}\%$  of the total inclusive cross section, then we predict a rate of  $1.0 \times 10^{-5}$  for the neutrino trimuon production relative to the single muon inclusive rate. This means that approximately 30% of all trimuon events are the product of  $c\bar{c}$  decays. We should note that this component is not present in the hadronic model used previously, since the low-mass pairs originate from the decays of low-mass vector ( $\rho, \omega, \phi$ ) and pseudo-scalar ( $\eta$ ) particles. The measured invariant mass of the  $\mu^+\mu^-$  pair seen in hadronic collisions falls rapidly in the region between 1 and 3 GeV, so this region does not make any significant contribution to the hadronic model. Hence, it is reasonable to add the  $c\bar{c}$  component to the

TABLE I. Comparison of the average values for the single-muon inclusive reaction reported by Haatuft *et al.*, with the predictions of our structure functions.

Variable	Experiment	Model
$\langle E_\nu \rangle$ (GeV)	$39.5 \pm 0.5$	42.1
$\langle E_\mu \rangle$ (GeV)	$22.6 \pm 0.4$	24.3
$\langle \nu \rangle$ (GeV)	$15.92 \pm 0.3$	17.9
$\langle Q^2 \rangle$ [(GeV/c) <sup>2</sup> ]	$6.96 \pm 0.2$	7.9
$\langle W \rangle$ (GeV/c)	$4.5 \pm 0.04$	4.6
$\langle x \rangle$	$0.24 \pm 0.003$	0.25
$\langle y \rangle$	$0.41 \pm 0.008$	0.41

TABLE II. Comparison of the average values for the  $\mu^-e^-$  events reported by Haatuft *et al.* for  $p_e > 0.5$  GeV/c with the predictions of the  $c\bar{c}$  model.

Variable	Experiment	Model
$\langle E_\nu \rangle$ (GeV)	$38.1 \pm 6.2$	43.2
$\langle E_\mu \rangle$ (GeV)	$17.1 \pm 4.0$	22.9
$\langle E_e \rangle$ (GeV)	$1.0 \pm 0.1$	3.0
$\langle \nu \rangle$ (GeV)	$20.1 \pm 3.1$	20.3
$\langle Q^2 \rangle$ [(GeV/c) <sup>2</sup> ]	$8.6 \pm 1.8$	9.2
$\langle W \rangle$ (GeV/c)	$5.4 \pm 0.6$	5.4
$\langle x \rangle$	$0.26 \pm 0.06$	0.26
$\langle y \rangle$	$0.56 \pm 0.06$	0.47
$\langle Z_e \rangle$	$0.06 \pm 0.01$	0.14
$\langle \phi_{\mu e} \rangle$	$104.3^\circ \pm 20^\circ$	$110.0^\circ$

contributions from the electromagnetic and hadronic models.

At this point it is appropriate to comment on the  $c\bar{c}$  model prediction for neutrino-induced  $\mu^-e^-$  events. We find that  $\nu N \rightarrow \mu^-e^-X$  has a rate of  $1 \times 10^{-4}$  with respect to the muon inclusive rate for cuts  $p_e > 0.3$  GeV/c,  $p_\mu > 4.5$  GeV/c, and  $m_{ee} > m_\pi$ . This number is lower than the measured rate of  $(3.1 \pm 1.9) \times 10^{-4}$  reported by Haatuft *et al.*<sup>2</sup> This is explained by the fact that the three *light-mass* pairs seen by them originate from other hadronic or electromagnetic sources. In fact, one of us<sup>12</sup> has already shown that the hadronic rate for  $\mu^-e^-$  events is approximately  $5 \times 10^{-4}$  of the charged-current rate for the cuts given above. The electromagnetic contribution was shown to be a factor of 10 smaller. Of the three events reported on Ref. 2, one has a value for  $\phi_{1(2+3)}$  of  $25^\circ$  and could be of electromagnetic origin, whereas the other two have large values of  $178^\circ$  and  $176^\circ$ , respectively, which is consistent with a hadronic interpretation. Our conclusion, therefore, is that these events are not likely to be the products of  $c\bar{c}$  decays but rather their existence confirms the magnitude of the other trilepton production mechanisms.

#### IV. MODEL FOR THE $\mu^-e^-$ EVENTS

We now turn our attention to the  $\mu^-e^-$  channel. The rates and distributions for these events follow from the same  $c\bar{c}$  production and decay model. All we have to do is change the initial neutrino spectrum and the cuts on the final leptons to agree with those of Haatuft *et al.* Hence, we use the 350-GeV CERN wide-band neutrino spectrum and a cut on the primary muon momentum at 4.5 GeV/c. The experimental group have found 13 good  $\mu^-e^-$  events with  $p_e > 0.3$  GeV/c, 10 of which have  $p_e > 0.5$  GeV/c and 7 have  $p_e > 0.8$  GeV/c. Since there is a large background which falls off rapidly with increasing  $p_e$ , the correction for missed events is large. After a careful study of event losses and backgrounds, they corrected the number of observed events for the electron detection probability and gave rates for the cases  $p_e > 0.5$  GeV/c and  $p_e > 0.8$  GeV/c, namely,

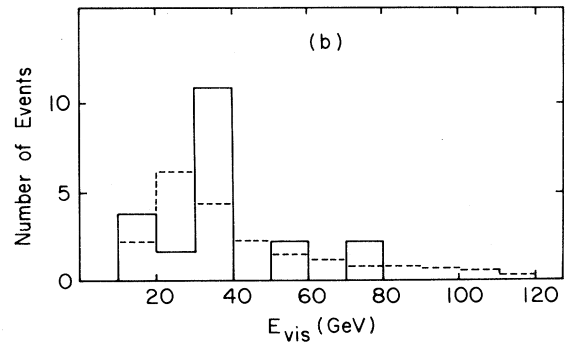
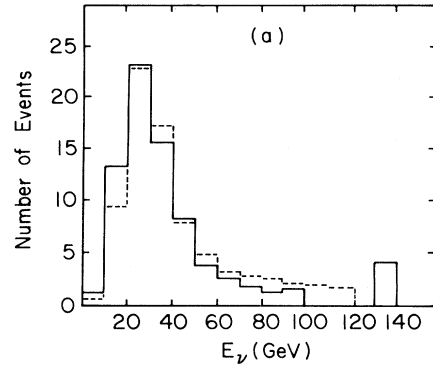


FIG. 7. The neutrino energy spectrum for (a) the charged-current events and (b) the  $\mu^-e^-$  events. The solid histograms show the experimental data and the dashed histograms show our results. The same notation is used in all the remaining figures.

$$\frac{\sigma(\nu_\mu N \rightarrow \mu^-e^-X)}{\sigma(\nu_\mu N \rightarrow \mu^-X)} = \begin{cases} (6.7 \pm 3.9) \times 10^{-4}, & p_e > 0.5 \text{ GeV}/c, \\ (5.3 \pm 2.9) \times 10^{-4}, & p_e > 0.8 \text{ GeV}/c. \end{cases}$$

We have calculated the signal for  $p_e > 0.5$  GeV/c to be  $6.5 \times 10^{-4}$ , which is in excellent agreement with their number. Cross sections for  $\sigma(\mu^-e^-)/\sigma(\mu^-)$  with and without cuts are shown in Fig. 6.

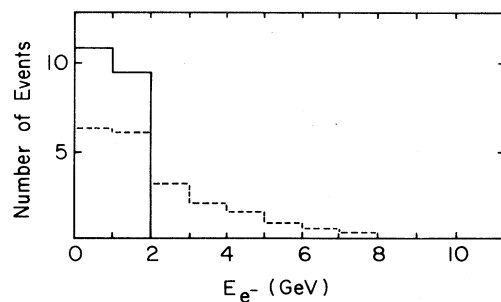


FIG. 8. The energy distribution of the electron in the  $\mu^-e^-$  events.

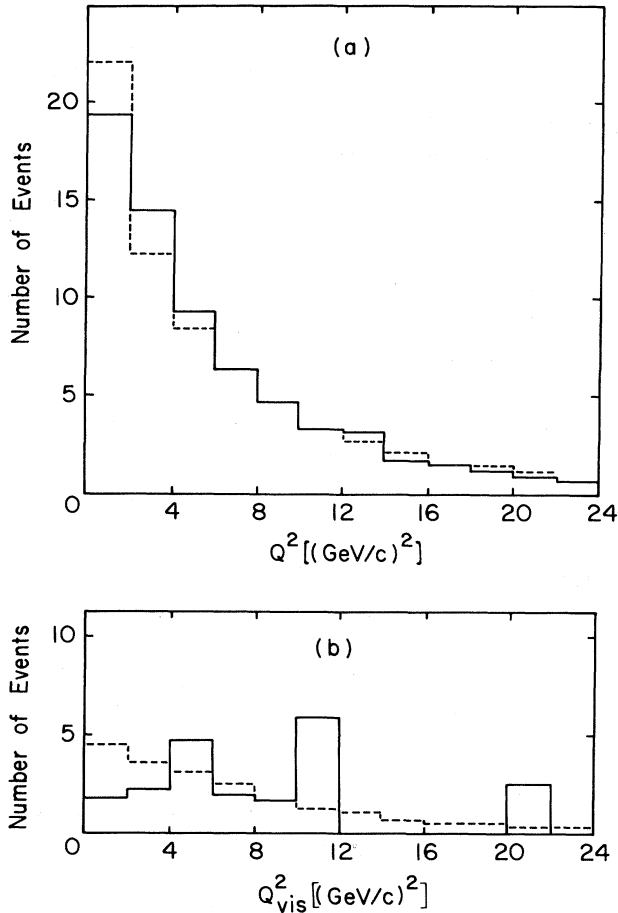


FIG. 9. (a) The  $Q^2$  distribution for the charged-current events and (b) the  $Q^2_{\text{vis}}$  distribution for the  $\mu^-e^-$  events.

Haatuft *et al.* also gave kinematical distributions for the corrected  $\mu^-e^-$  events with a  $p_e$  cut at 0.5 GeV/c. The effect of the correction efficiency is to increase the number of events so the histograms no longer contain an integer number. This yields approximately 21 corrected  $\mu^-e^-$  events. The  $\mu^-e^-$  histograms were then compared with corresponding results on single  $\mu^-$  and  $\mu^-e^+$  events. We simply assume that they found exactly 21  $\mu^-e^-$  events and show our predictions for the distributions of the same-sign dileptons. To check that our quark distribution functions are valid, we also compare our theoretical distributions for the single  $\mu^-$  events with the experimental data.

First of all, we give a list of all the averages for the single  $\mu^-$  inclusive data in Table I and for the  $\mu^-e^-$  events in Table II. The reasons for the small discrepancies are clear when we examine the respective plots. Even though the number of events is small, we do show the actual distributions as a cross check of the model and a prediction for future experiments. In Fig. 7(a), we show the  $E_\nu$  spectrum for the charged-current events (solid curves) and

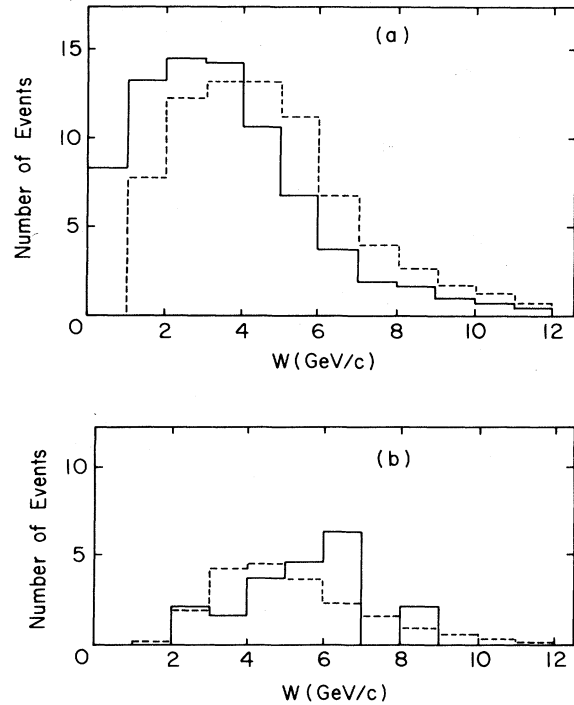


FIG. 10. The  $W$  distribution for (a) the charged-current events and (b) the  $\mu^-e^-$  events.

compare them with our predictions (dashed curves). We reconstruct a visible energy spectrum,  $E_{\text{vis}}$ , for the  $\mu^-e^-$  events in the  $c\bar{c}$  model by neglecting the energy of the missing neutrino. This is compared with the experimental data in Fig. 7(b). In both cases, there is reasonable agreement between theory and experiment.

In Fig. 8, we show the  $E_e$  energy spectrum. Our model predicts a higher  $\langle E_e \rangle$  than the data. However, this disagreement may be a reflection of an experimental bias because high-energy electrons tend to radiate easily so their energy should actually be larger. Therefore, it is not clear how seriously to take the results in Fig. 8. We only note that the  $\mu^-e^+$  events, which are not shown here, have also a larger number of low-energy positron events (between 0.3 and 0.5 GeV/c) than expected from the decay of a single charged particle.

Figure 9 shows the  $Q^2$  distribution for the charged-current events and the  $Q^2_{\text{vis}}$  distribution for the  $\mu^-e^-$  events. In Fig. 10(a), we show the  $W$  distribution for the charged-current events. Our structure functions have been chosen to fit the data in the deep-inelastic region only so we find no events below 1 GeV and very few below 2 GeV. The data have not been cut to eliminate small- $W$  events so the experimental value of  $\langle W \rangle$  is lower than the theoretical one. Figure 10(b) shows the same distribution for the  $\mu^-e^-$  events. We have not tried to construct a better fit to the original  $W$  distribution because such small changes are not going to alter our results significantly. Next we

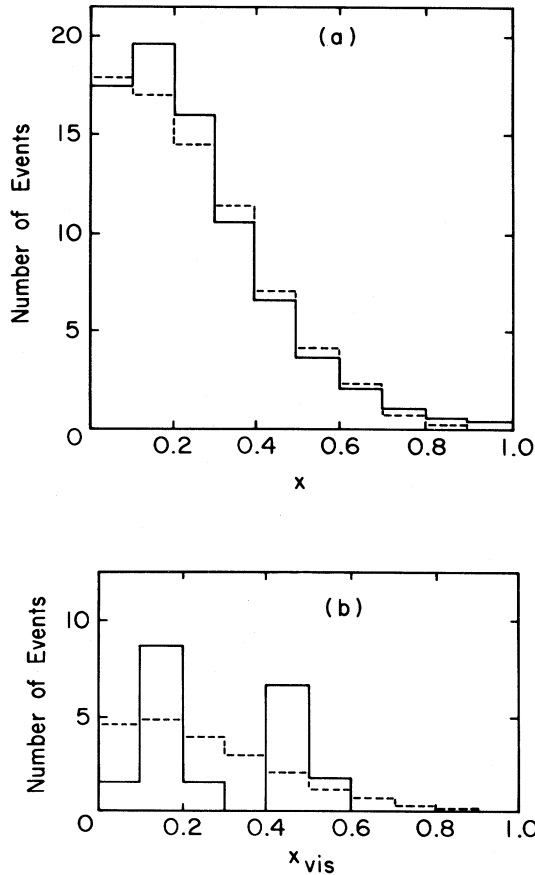


FIG. 11. The  $x$  distribution for (a) the charged-current events and the  $x_{\text{vis}}$  distribution for (b) the  $\mu^-e^-$  events.

show the  $x$  and  $y$  distributions for the  $\mu^-$  inclusive events in Figs. 11(a) and 12(a). The corresponding  $x_{\text{vis}}$  and  $y_{\text{vis}}$  distributions are given in Figs. 11(b) and 12(b). Figure 13 shows the distribution in  $z_e = E_e/(\nu + M)$  for the  $\mu^-e^-$  events. Finally, in Fig. 14, we show the distributions in the azimuthal opening angle between the  $\mu^-$  and the  $e^-$  in the plane perpendicular to the neutrino beam.

Within the limitations of the data, we see there is reasonable agreement between theory and experiment. The only disturbing fact is that no  $V^0$  candidates were seen in the  $\mu^-e^-$  events. This is not due to experimental biases since the same group found  $V^0$  candidates in their sample of  $\mu^-e^+$  events. In fact, they quote

$$\frac{\sigma(\nu_\mu N \rightarrow \mu^- e^+ K^0(\Lambda^0) X)}{\sigma(\nu_\mu N \rightarrow \mu^- e^- X)} = 1.1 \pm 0.4.$$

The lack of  $V^0$  candidates may be a statistical effect. It is fortunate that the Columbia-BNL group have conducted an experimental run at Fermilab and are analyzing their film to find  $\mu^-e^-$  events. We hope that there will shortly

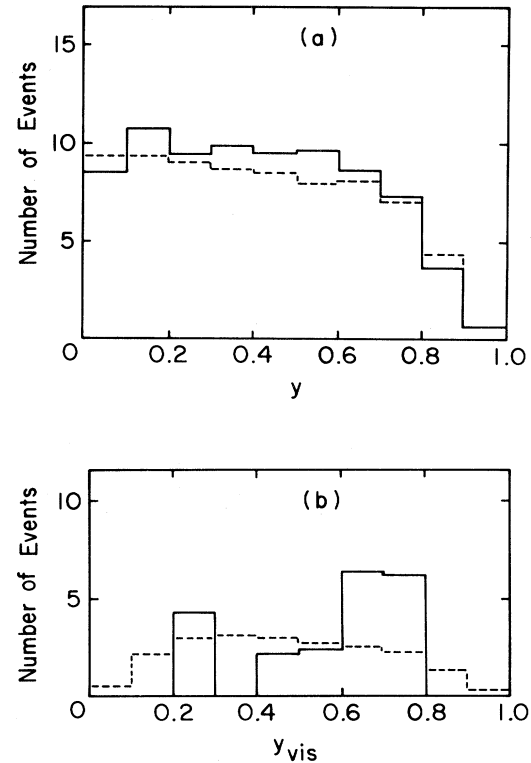


FIG. 12. The  $y$  distribution for (a) the charged-current events and the  $y_{\text{vis}}$  distribution for (b) the  $\mu^-e^-$  events.

be an answer to the  $V^0$  question.

We finish this section with a comment on antineutrino production of  $\mu^+e^+$  events. After switching to the antineutrino spectrum used by Ammosov *et al.*<sup>3</sup> and changing the sign of the  $F_3$  structure function, we have calculat-

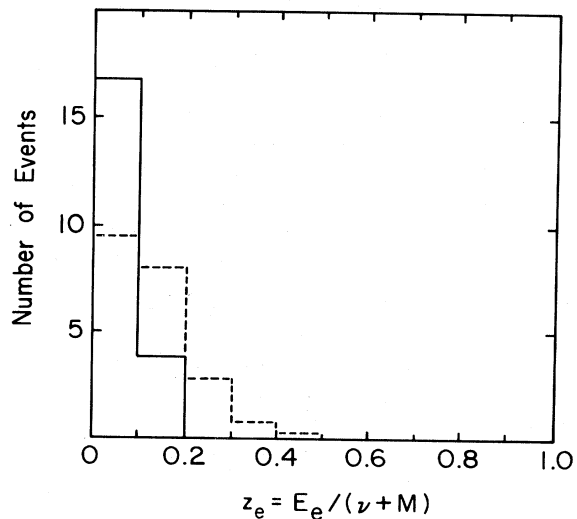


FIG. 13. The  $z_e$  distribution for the  $\mu^-e^-$  events.



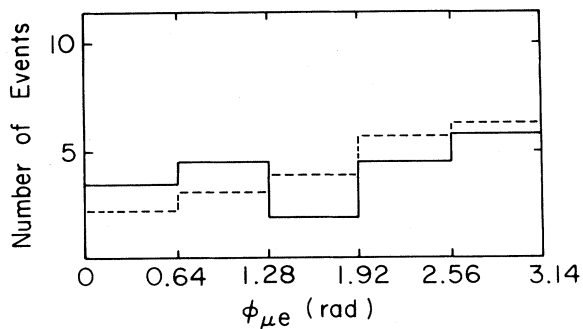


FIG. 14. The  $\phi_{\mu e}$  distribution for the  $\mu^-e^-$  events.

ed the rate for  $\mu^+e^+$  events satisfying their cuts of  $E_\mu > 4$  GeV and  $E_e > 0.4$  GeV. We find

$$\frac{\sigma(\bar{\nu}_\mu N \rightarrow \mu^+e^+X)}{\sigma(\bar{\nu}_\mu N \rightarrow \mu^+X)} = 6 \times 10^{-4}$$

which agrees well with their rate of  $(4.8_{-3.2}^{+5.3}) \times 10^{-4}$ .

## V. CONCLUSION

The phenomenological  $c\bar{c}$  production and decay model of Godbole and Roy has been shown to give a satisfactory explanation of the rate and distributions for the  $\mu^-e^-$  events seen by Haatuft *et al.*<sup>2</sup> It also accounts for the rate of antineutrino-induced  $\mu^+e^+$  events. Approximately 30% of all neutrino-induced  $\mu^-e^+\mu^-$  events seem, therefore, to arise from the same source. Hence, the correlations between multileptons which are expected from a  $c\bar{c}$  model are found in the data.

## ACKNOWLEDGMENTS

J. Smith would like to thank M. Willutzky for discussions of the  $\mu^-e^-$  events. He would also like to thank B. Peyaud, K. Kleinknecht, and H. Willutzki for discussions of the CDHS data. This work was supported in part by NSF Contract No. PHY 81-09110.

- <sup>1</sup>A. Benvenuti *et al.*, Phys. Rev. Lett. **35**, 1199 (1975); B. C. Barish *et al.*, *ibid.* **36**, 939 (1976); M. Holder *et al.*, Phys. Lett. **70B**, 396 (1977); A. Benvenuti *et al.*, Phys. Rev. Lett. **41**, 725 (1977); **41**, 1204 (1977); J. G. H. de Groot *et al.*, Phys. Lett. **86B**, 103 (1979); M. Jonker *et al.*, *ibid.* **107B**, 241 (1981); T. Trinko *et al.*, Phys. Rev. D **23**, 1889 (1981); N. Nishikawa *et al.*, Phys. Rev. Lett. **46**, 1555 (1981).
- <sup>2</sup>A. Haatuft, K. Myklebost, J. M. Olsen, M. Willutzky, and P. Petitjean, Report No. CERN-EP 83/16 (unpublished).
- <sup>3</sup>V. V. Ammosov *et al.*, Phys. Lett. **106B**, 151 (1981).
- <sup>4</sup>F. Bletzacker, H. T. Nieh, and A. Soni, Phys. Rev. Lett. **38**, 1241 (1977); F. Bletzacker and H. T. Nieh, Report No. ITP-SB-77-42 (unpublished); H. Goldberg, Phys. Rev. Lett. **39**, 1598 (1977); B. L. Young, T. F. Walsh, and T. C. Yang, Phys. Lett. **74B**, 111 (1978); V. Barger, T. Gottschalk, and R. J. N. Phillips, Phys. Rev. D **18**, 2308 (1978); Z. Hioki, Prog. Theor. Phys. **60**, 1094 (1978); G. L. Kane, J. Smith, and J. A. M. Vermaseren, Phys. Rev. D **19**, 1978 (1979); J. Smith and C. H. Albright, Phys. Lett. **85B**, 119 (1979); R. J. N. Phillips, Nucl. Phys. **B153**, 475 (1979); S. D. Brodsky, P. Hoyer, C. Peterson, and N. Sakai, Phys. Lett. **93B**, 451 (1980); S. D. Brodsky, C. Peterson, and N. Sakai, Phys. Rev. D **23**, 2745 (1981); K. Hagiwara, Nucl. Phys. **B173**, 487 (1980); V. Barger, W. Y. Keung, and R. J. N. Phillips, Phys. Rev. D **24**, 244 (1981); **25**, 1803 (1982).
- <sup>5</sup>R. M. Godbole and D. P. Roy, Phys. Rev. Lett. **48**, 1711 (1982).
- <sup>6</sup>B. L. M. Peyaud, in *Current Hadron Interactions*, proceedings of the XIVth Rencontre de Moriond, Les Arcs, Savoie, France, 1979, edited by J. Trân Thanh Vân (Editions Frontières, Dreux, France, 1979), p. 485; J. Smith, *ibid.*, p. 631; J. J. Murtagh, in *Proceedings of the 9th International Symposium on Lepton and Photon Interactions at High Energy, Fermilab*, 1979, edited by T. B. W. Kirk and H. D. I. Abarbanel (Fermilab, Batavia, Illinois, 1980), p. 277; H. J. Willutzki, in *Neutrino 79*, Proceedings of the International Conference on Neutrinos, Weak Interactions and Cosmology, Bergen, Norway, 1979, edited by A. Haatuft and C. Jarlskog (University of Bergen, Bergen, 1980), p. 92; J. Smith, *ibid.*, p. 101; M. H. Shaevitz, in *The Weak Interactions*, proceedings of the Summer Institute on Particle Physics, edited by A. Mosher (SLAC, Stanford, 1980); B. L. M. Peyaud *et al.*, in *Proceedings of the 1981 International Conference on High Energy Physics, Lisbon, 1981*, edited by J. Dias de Deus and J. Soffer (European Physical Society, Romania, 1982) p. 714; H. E. Fisk, in *Proceedings of the 1981 International Symposium on Lepton and Photon Interactions at High Energies, Bonn*, edited by W. Pfeil (Physikalisches Institut, Universität Bonn, Bonn, 1981), p. 703; J. Knobloch, in *Neutrino 81*, proceedings of the International Conference on Neutrino Physics and Astrophysics, Maui, Hawaii, 1981, edited by R. J. Cence, E. Ma, and A. Roberts (University of Hawaii High Energy Physics Group, Honolulu, 1981), p. 421; J. V. Allaby, *ibid.*, p. 429; M. Willutzky, *ibid.*, p. 442; T. Y. Ling, *ibid.*, p. 449; K. Kleinknecht, in *Proceedings of the 10th International Conference on Neutrino Physics and Astrophysics, Balatonfüred, Hungary, 1982*, edited by A. Frenkel and L. Jenik (Roland Eötvös University, Budapest, Hungary, 1982), p. 115; F. Halzen, in *Proceedings of the 21st International Conference on High Energy Physics, Paris, 1982*, edited by P. Petiau and M. Porneuf [J. Phys. (Paris) Colloq. **43**, C3-381 (1982)]; V. Barger, *ibid.*, **43**, C3-32 (1982).
- <sup>7</sup>B. C. Barish *et al.*, Phys. Rev. Lett. **38**, 577 (1977); **40**, 432 (1977); **40**, 498 (1977); A. Benvenuti *et al.*, *ibid.* **38**, 1110 (1977); M. Holder *et al.*, Phys. Lett. **70B**, 393 (1977); J. G. H. de Groot *et al.*, *ibid.* **85B**, 131 (1979).
- <sup>8</sup>T. Hansl *et al.*, Phys. Lett. **77B**, 114 (1978); Nucl. Phys. **B142**, 381 (1978).
- <sup>9</sup>B. Peyaud, Ph. D. thesis, University of Paris VII, 1981 (unpublished).
- <sup>10</sup>V. Barger, T. Gottschalk, and R. J. N. Phillips, Phys. Rev. D **18**, 2308 (1978).
- <sup>11</sup>J. Smith and J. A. M. Vermaseren, Phys. Rev. D **17**, 2288 (1978); V. Barger, T. Gottschalk, and R. J. N. Phillips, *ibid.* **17**, 2284 (1978); R. M. Barnett, L. N. Chang, and N. Weiss, *ibid.* **17**, 2266 (1978).
- <sup>12</sup>J. Smith, Nucl. Phys. **B157**, 451 (1979).